Field-induced quantum phase transition in the anisotropic Kondo necklace model

P. Thalmeier[1] and A. Langari[2]
[1]*Max Planck Institute for Chemical Physics of Solids, 01187 Dresden, Germany*
[2]*Physics Department, Sharif University of Technology, Tehran 11365-9161, Iran*
(Received 4 December 2006; revised manuscript received 8 March 2007; published 18 May 2007)

The anisotropic Kondo necklace model in two and three dimensions is treated as a genuine model for magnetic to Kondo singlet quantum phase transitions in the heavy fermion compounds. The variation of the quantum critical point with anisotropy parameters has been investigated previously in the zero-field case. Here, we extend the treatment to finite fields using a generalized bond operator representation including all triplet states. The variation of critical t_c with magnetic field and the associated phase diagram is derived. The influence of anisotropies and the different g factors for localized and itinerant spins on the field dependence of t_c is also investigated. It is found that three different types of behavior may appear: (i) destruction of antiferromangetism and appearance of a singlet state above a critical field, (ii) the inverse behavior, namely, field-induced antiferromagnetism out of the Kondo singlet phase, and (iii) reentrance behavior of the Kondo singlet phase as a function of field strength.

DOI: 10.1103/PhysRevB.75.174426 PACS number(s): 75.10.Jm, 75.30.Mb

I. INTRODUCTION

Kondo-necklace- (KN-) type models are useful to discuss the quantum phase transitions between Kondo singlet and antiferromagnetically ordered states such as found in heavy fermion compounds.[1–5] They were originally proposed by Doniach[6] for the one-dimensional case as a simplified version of the itinerant Kondo lattice (KL) models.[7] Thereby, the kinetic energy of conduction electrons is replaced by an intersite exchange term. For a pure xy-type intersite exchange, this may be obtained by a Jordan-Wigner transformation. However, at higher D the replacement cannot be justified easily. The intuitive argument is that at low temperatures the charge fluctuations in the Kondo lattice model are frozen out and the remaining spin fluctuation spectrum can be simulated by an antiferromagnetic intersite interaction term of immobile $\boldsymbol{\tau}$ spins coupled by a Kondo interaction to the local noninteracting spins $\mathbf{S}$. Recent exact-diagonalization studies of finite clusters for both Kondo lattice and Kondo necklace models have indeed found that the competitions between on-site Kondo singlet formation and antiferromagnetic (AF) intersite correlations are very similar in both models.[8,9] A more formal way to get rid of charge fluctuations in the KL model is an inclusion of a Hubbard term for conduction electrons (KLU model) which leads to the isotropic KN model in the large-U limit at half filling.

Nevertheless, one should consider the Kondo necklace model for $D \geqslant 2$ as a model in its own right which is suitable for studying quantum phase transitions between a Kondo singlet (KS) and an AF phase. In its original form the local Kondo exchange is isotropic while the intersite exchange is of xy type. This model has U(1) symmetry. Later, more general models with arbitrary anisotropy of Kondo as well as intersite exchange terms have been considered.[10] Indeed, compounds which exhibit the KS to AF quantum phase transition have mostly uniaxial symmetries. A full account of the influence of uniaxial anisotropies of both terms in the Kondo necklace Hamiltonian on the quantum critical point has been given in Ref. 11. The $D=2$ KN model without any anisotropy may also be understood as a special case of a bilayer Heisenberg model[12,13] where the intersite bonds are cut in one of the layers. A reintroduction of holes in this case leads to the KNtJ model which is related to the KLU model away from half filling.[13,14]

In the general anisotropic KN model, the quantum phase transition is achieved by varying the ratio of "hopping" t—i.e., the intersite interactions of $\boldsymbol{\tau}$ spins to the on-site Kondo interaction J. In practice this is achieved by varying pressure (hydrostatic or chemical). An alternative way to arrive at the QCP is to apply an external magnetic field which breaks the local Kondo singlets and leads to a field dependence of the critical t_c. Starting from a noncritical or above critical t at zero field, the system may then be tuned to the QCP by varying the field strength. This is indeed a practical method frequently applied.[15] To investigate field-induced quantum phase transitions from a Kondo-singlet to AF-ordered state or vice versa we have extended our previous work to include the effect of the magnetic field within the Kondo necklace model. However, this introduces an additional parameter: namely, the ratio of effective g factors for the local Kondo spins and the interacting spins. They can be different due to the different strength of spin-orbit coupling and crystalline electric field effects involved in the formation of the $\boldsymbol{\tau}$ and $\mathbf{S}$ (pseudo)spins. A mainly numerical study of the itinerant isotropic KL model in a magnetic field has been given previously.[16]

In Sec. II we define the anisotropic KN model in a magnetic field and in Sec. III briefly discuss the local state space of the Kondo term in an external field. In Sec. IV, we perform the transformation from spin to bosonic variables and in Sec. V derive the self-consistent equations for the mean-field boson condensate amplitudes in the singlet and antiferromagnetic phases. The influence of higher-order terms in the Hamiltonian is discussed in Sec. VI. In Sec. VII, we investigate the numerical solutions and discuss the resulting quantum critical t-h phase diagram. A discussion is provided in Sec. VIII, and Sec. IX finally gives the conclusions.

 ©2007 The American Physical Society

II. ANISOTROPIC KONDO NECKLACE MODEL IN AN EXTERNAL FIELD

To investigate field-induced quantum critical behavior, we start from the anisotropic KN model with U(1) symmetry[11] where the field is applied along the anisotropy (z) direction:

$$\mathcal{H} = \mathcal{H}_t + \mathcal{H}_J + \mathcal{H}_Z = t \sum_{\langle n,m \rangle} (\tau_n^x \tau_m^x + \tau_n^y \tau_m^y + \delta \tau_n^z \tau_m^z) + J \sum_n (\tau_n^x S_n^x + \tau_n^y S_n^y + \Delta \tau_n^z S_n^z) + \gamma \sum_i S_n^z + \gamma' \sum_i \tau_n^z. \quad (1)$$

Here, the summation over nearest neighbors (NN) is indicated by brackets and τ_n^α is the α component ($\alpha = x, y, z$) of the "itinerant" electron spin at site n, whereas S_n^α is the α component of localized spins at position n. For the exchange coupling between the itinerant and localized spins, we generally use $J_x \equiv J$ as reference energy scale in all figures except when stated otherwise. The local anisotropy parameter Δ is defined by the relation $J_z = \Delta J_x$ between the z-axis and in-plane (xy) local exchange. The hopping parameter of the itinerant electrons is proportional to t with the anisotropy in the z direction given by δ. The present model has three control parameters: t/J_x and the anisotropy parameters (δ, Δ). In the Zeeman term, we defined $\gamma = -g_s h$ and $\gamma' = -g_\tau h$ with $h = \mu_B H$ where H is the strength of the applied field. Furthermore, g_s and g_τ are the gyromagnetic ratios for localized (S_n^α) and itinerant (τ_n^α) spins, respectively. They are determined by the combined effect of spin-orbit coupling and crystalline electric fields which depends on the degree of localization or itineracy of electrons. Therefore g_s and g_τ in general need not be equal. We shall consider two extreme cases: namely, $(g_s, g_\tau) = (2,0)$ and $(g_s, g_\tau) = (2,2)$. The former is more realistic, since in real heavy fermion compounds most of the magnetic response is due to the localized electrons with pseudospin $\mathbf{S}$. As in previous work,[11,17] the present study of field-induced quantum phase transitions in the anisotropic KN model is based on the bond operator formulation. Its Hilbert space is spanned by local singlet-triplet states of $(\mathbf{S}_n, \boldsymbol{\tau}_n)$ spin dimers represented by bosonic degrees of freedom. In applying this technique to the finite-field case, we will largely use the same or similar notations as in the previous zero-field case[11] for consistency.

III. LOCAL LEVELS AND ZEEMAN SPLITTING

Before we perform the transformation to bosonic variables, it is useful to have a clear understanding of the local singlet-"triplet" level scheme as a function of anisotropy and magnetic field because certain tendencies of the quantum critical behavior are correlated with the splitting of the ground state and the first excited state of a local bond. Therefore, we first diagonalize the local Hamiltonian $\mathcal{H}_L = \mathcal{H}_J + \mathcal{H}_Z$. This leads to eigenvalues $\epsilon_i = E_i/(J_x/4)(i = 1-4)$ given by

$$\epsilon_{1,2} = \Delta \pm \hat{\gamma}_+,$$

$$\epsilon_{3,4} = \pm (4 + \hat{\gamma}_-^2)^{1/2} - \Delta,$$

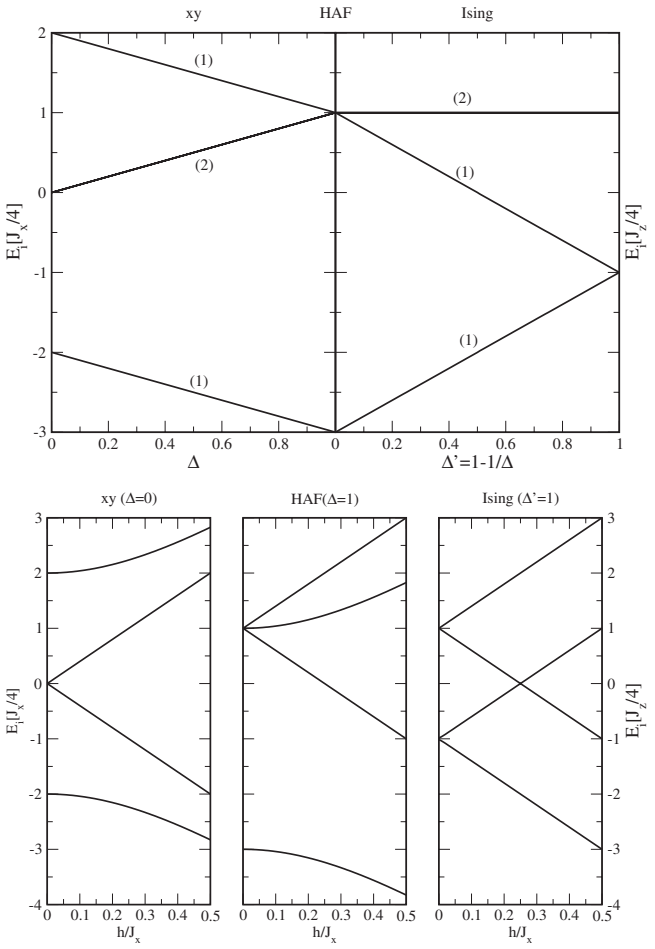

FIG. 1. Top: dependence of local energy levels after Eq. (2) on the local anisotropy Δ (xy side) or $\Delta' = 1 - 1/\Delta$ (Ising side) at zero field. Numbers in parentheses denote the degeneracy of each level. Bottom: field dependence ($h = \mu_B H$) of local energy level for three extreme cases. Note that in the xy case the excitation energy from ground state to first excited state vanishes asymptotically ($h \gg J_x$), whereas in the other cases it reaches a constant (HAF) or is equal to a constant (Ising). Here, we used $(g_s, g_\tau) = (2,0)$.

$$\hat{\gamma}_\pm = -\frac{h}{(J_x/4)} \frac{1}{2}(g_s \pm g_\tau) \equiv \frac{\gamma_\pm}{(J_x/4)}, \quad (2)$$

with $\gamma_\pm = \frac{1}{2}(\gamma \pm \gamma') = -g_\pm h$ and $g_\pm = \frac{1}{2}(g_s \pm g_\tau)$. Defining $S_z^t = \tau_z + S_z$, then $\epsilon_{1,2}$ are the energies of the triplet states $|\uparrow\uparrow\rangle$, $|\downarrow\downarrow\rangle$ with $S_z^t = \pm 1$, respectively, which exhibit the linear Zeeman effect. Furthermore, $\epsilon_{3,4}$ correspond to the triplet $S_z^t = 0$ state $\frac{1}{\sqrt{2}}(|\uparrow\downarrow\rangle + |\downarrow\uparrow\rangle)$ and singlet state $\frac{1}{\sqrt{2}}(|\uparrow\downarrow\rangle - |\downarrow\uparrow\rangle)$, respectively. They show level repulsion in a magnetic field, except for $g_s = g_\tau$ when the total S_z^t component is conserved and commutes with $\mathcal{H}_L$. It is obvious that the spectrum of eigenstates in Eq. (2) is invariant under the transformation $(g_s, g_\tau) \to (g_\tau, g_s)$. The variation of zero-field energy levels with Δ is shown in Fig. 1 (top) from the xy-U(1) limit ($\Delta = 0$) via the Heisenberg SU(2) point ($\Delta = 1$) to the Ising Z_2 limit ($\Delta = \infty$). The field dependence for a few selected Δ values and g factors $(g_s, g_\tau) = (2,0)$ is shown in Fig. 1 (bottom). For $(g_s, g_\tau) = (2,2)$ (not shown in Fig. 1) the ground-state and

first excited-state levels cross at $h_{cr}/J_x=0.25,0.50$ for $(\delta,\Delta)=(0,0)$ and (1,1), respectively. In such a case one may expect that the quantum critical $t_c(h_{cr})$ for the transition from the Kondo singlet to AF phase vanishes.

IV. DERIVATION OF EFFECTIVE BOSONIC MODEL

We apply the transformation from spin variables (S_α,τ_α) to bond variables (s,t_α) $(\alpha=x,y,z)$ to the Hamiltonian in Eq. (1). It is given by[18]

$$S_{n,\alpha}=\frac{1}{2}(s_n^\dagger t_{n,\alpha}+t_{n,\alpha}^\dagger s_n-i\epsilon_{\alpha\beta\gamma}t_{n,\beta}^\dagger t_{n,\gamma}),$$

$$\tau_{n,\alpha}=\frac{1}{2}(-s_n^\dagger t_{n,\alpha}-t_{n,\alpha}^\dagger s_n-i\epsilon_{\alpha\beta\gamma}t_{n,\beta}^\dagger t_{n,\gamma}), \tag{3}$$

where $\epsilon_{\alpha\beta\gamma}$ is the fully antisymmetric tensor. By construction, the singlet (s) and triplet (t_α) operators generate the local eigenstates of $\mathcal{H}_L$ for zero field and no anisotropy:[19]

$$s^\dagger|0\rangle=\frac{1}{\sqrt{2}}(|\uparrow\downarrow\rangle-|\downarrow\uparrow\rangle),\quad t_x^\dagger|0\rangle=-\frac{1}{\sqrt{2}}(|\uparrow\uparrow\rangle-|\downarrow\downarrow\rangle),$$

$$t_z^\dagger|0\rangle=\frac{1}{\sqrt{2}}(|\uparrow\downarrow\rangle+|\downarrow\uparrow\rangle),\quad t_y^\dagger|0\rangle=\frac{i}{\sqrt{2}}(|\uparrow\uparrow\rangle+|\downarrow\downarrow\rangle). \tag{4}$$

Here, the first and second arrows indicate the z component of $\boldsymbol{\tau}$ and $\mathbf{S}$ spins, respectively. The singlet and triplet operators satisfy the usual bosonic commutation relations according to

$$[s_n,s_n^\dagger]=1,\quad [t_{n,\alpha},t_{n,\beta}^\dagger]=\delta_{\alpha,\beta},\quad [s_n,t_{n,\beta}^\dagger]=0. \tag{5}$$

All other commutators vanish. The physical states have to satisfy the local constraint $s_n^\dagger s_n+\Sigma_\alpha t_{n,\alpha}^\dagger t_{n,\alpha}=1$. This transformation leads to an effective Hamiltonian in terms of singlet (s) and triplet (t_α) bosons. It has been argued in Refs. 11 and 17 that one may restrict oneself to the terms which are bilinear in the triplet bosons and we will later in Sec. VI discuss to what extent this is justified. For the moment we restrict ourselves to the bilinear contribution. It can be written as the sum of a local term $\mathcal{H}_L$ and an intersite interaction term $\mathcal{H}_1$. Here

$$\mathcal{H}_L=\mathcal{H}_J+\mathcal{H}_Z=\frac{J_x}{4}\sum_n[-(2+\Delta)s_n^\dagger s_n+(2-\Delta)t_{n,z}^\dagger t_{n,z}+\Delta(t_{n,x}^\dagger t_{n,x}+t_{n,y}^\dagger t_{n,y})]+\gamma_-\sum_n(s_n^\dagger t_{nz}+t_{nz}^\dagger s_n)-i\gamma_+\sum_n(t_{nx}^\dagger t_{ny}-t_{ny}^\dagger t_{nx}), \tag{6}$$

contains the on-site Kondo interaction $(\mathcal{H}_J)$ and the Zeeman term $(\mathcal{H}_Z)$. The bilinear interaction term is given by

$$\mathcal{H}_1^{(2)}=\frac{t}{4}\sum_{\langle n,m\rangle}\sum_{\alpha=x,y}[s_n^\dagger t_{n,\alpha}(s_m^\dagger t_{m,\alpha}+t_{m,\alpha}^\dagger s_m)+\text{H.c.}]+\frac{t\delta}{4}\sum_{\langle n,m\rangle}[s_n^\dagger t_{n,z}(s_m^\dagger t_{m,z}+t_{m,z}^\dagger s_m)+\text{H.c.}]. \tag{7}$$

The physical constraint on the local Hilbert space is enforced by adding a Lagrange term at each site with an associated chemical potential μ_n, leading to

$$\mathcal{H}=\mathcal{H}_L+\sum_n\mu_n\left(s_n^\dagger s_n+\sum_{\alpha=x,y,z}t_{n,\alpha}^\dagger t_{n,\alpha}-1\right)+\mathcal{H}_1^{(2)}\equiv\mathcal{H}_0+\mathcal{H}_1^{(2)}. \tag{8}$$

This Hamiltonian is diagonalized within a mean-field approximation for the bond-operator singlet and triplet bosons. We assume that in general there are three independent bosonic amplitudes which characterize the phases in the (t,h) plane: singlet $\bar{s}=\langle s_n\rangle$ denoting the strength of local singlet formation, staggered triplet $\bar{t}=\pm\langle t_{n,x}\rangle$ which determines the AF order parameter (polarized along x), and homogeneous triplet $t_0=\langle t_{n,z}\rangle$ which determines the magnetization caused by the external field along the z direction. For technical reasons, it is advantageous to transform to circularly polarized transverse triplet coordinates (u_n,d_n) with respect to the field direction (z axis). The transformation and its inverse are given by

$$u_n=-\frac{1}{\sqrt{2}}(t_{nx}-it_{ny}),\quad t_{nx}=-\frac{1}{\sqrt{2}}(u_n-d_n),$$

$$d_n=\frac{1}{\sqrt{2}}(t_{nx}+it_{ny}),\quad t_{ny}=-\frac{i}{\sqrt{2}}(u_n+d_n). \tag{9}$$

In circular triplet coordinates, the Hamiltonian may then be written as

$$\mathcal{H}_0=\sum_n\left[\left(-\frac{J_x}{4}(2+\Delta)+\mu_n\right)s_n^\dagger s_n+\left(\frac{J_x}{4}(2-\Delta)+\mu_n\right)t_{nz}^\dagger t_{nz}+\left(\frac{J_x}{4}\Delta+\gamma_++\mu_n\right)u_n^\dagger u_n+\left(\frac{J_x}{4}\Delta-\gamma_++\mu_n\right)d_n^\dagger d_n+\gamma_-(s_n^\dagger t_{nz}+t_{nz}^\dagger s_n)-\mu_n\right] \tag{10}$$

and

$$\mathcal{H}_1^{(2)}=-\frac{t}{4}\sum_{\langle n,m\rangle}\{[s_n^\dagger s_m^\dagger(u_nd_m+d_nu_m)+\text{H.c.}]-[s_n^\dagger s_m(u_nu_m^\dagger+d_nd_m^\dagger)+\text{H.c.}]\}+\frac{\delta t}{4}\sum_{\langle n,m\rangle}[(s_n^\dagger s_m^\dagger t_{nz}t_{mz}+\text{H.c.})+(s_n^\dagger s_m t_{nz}t_{mz}^\dagger+\text{H.c.})]. \tag{11}$$

Separating the mean values and the corresponding fluctuations the Fourier components of singlet and triplet operators are then given by

$$s_k=\sqrt{N}\bar{s},$$

$$u_k=\sqrt{N}\bar{u}\delta_{k,Q}+\hat{u}_k,$$

$$d_k=\sqrt{N}\bar{d}\delta_{k,Q}+\hat{d}_k,$$

$$t_{k,z} = \sqrt{N}\bar{t}_0\delta_{k,0} + \hat{t}_{k,z}. \tag{12}$$

Here we assumed that if AF order appears, it will be of the in-plane type ($\perp \hat{\mathbf{z}}, \mathbf{H}$). Therefore, the case of AF order will only be considered for $\delta \leqslant 1$. Instead of $\bar{t}_0$, it will later be convenient to use $\bar{\tau}_0$ which is defined by the relation $\bar{t}_0 = \bar{s}\bar{\tau}_0$. In the paramagnetic phase at zero field, only $\bar{s}$ will be different from zero with a value close to 1 (Ref. 11). As the field increases, $\bar{s}$ will decrease and simultaneously the triplet amplitude $\bar{t}_0$ associated with the uniform induced moment increases. If an AF transition occurs, $\bar{s}$ will further decrease and u,d will increase accordingly with the field. The constraint $\bar{s}^2 + \bar{t}_0^2 + (|\bar{u}|^2 + |\bar{d}|^2) \simeq 1$ is always respected for any field strength. In the limit $h/J_x \gg 1$, the amplitudes $\bar{s}$ and $\bar{t}_0$ become asymptotically equal. On the mean-field level, this signifies that the ground state of the local level scheme becomes an equal amplitude mixture of the two states with $S_z^t = 0$ which show the level repulsion in Fig. 1. Therefore, it is possible to use the zero-field singlet-triplet bosons in Eq. (3) as a basis even in the present finite-field problem. On the mean-field level, the physical constraint automatically takes care of the change in the local ground-state wave function. Inserting the above expressions into the Hamiltonian of Eqs. (10) and (11), one obtains a bilinear form in the triplet fluctuation operators $(\hat{u}_k, \hat{d}_k, \hat{t}_{kz})$ which may be diagonalized with two separate Bogoliubov transformations given for the z polarization by

$$a_k = \cosh(\theta_{k,z})\hat{t}_{k,z} + \sinh(\theta_{k,z})\hat{t}^\dagger_{-k,z},$$

$$a^\dagger_{-k} = \sinh(\theta_{k,z})\hat{t}_{k,z} + \cosh(\theta_{k,z})\hat{t}^\dagger_{-k,z} \tag{13}$$

and for the two circular polarized triplets by

$$A_k = \cosh(\theta_{k,\perp})\hat{u}_k + \sinh(\theta_{k,\perp})\hat{d}^\dagger_{-k},$$

$$B^\dagger_{-k} = \sinh(\theta_{k,\perp})\hat{u}_k + \cosh(\theta_{k,\perp})\hat{d}^\dagger_{-k},$$

$$B_k = \cosh(\theta_{k,\perp})\hat{d}_k + \sinh(\theta_{k,\perp})\hat{u}^\dagger_{-k},$$

$$A^\dagger_{-k} = \sinh(\theta_{k,\perp})\hat{d}_k + \cosh(\theta_{k,\perp})\hat{u}^\dagger_{-k}. \tag{14}$$

The transformation angles $\theta_{k,z}$ and $\theta_{k,\perp}$ are obtained from the diagonalization conditions

$$\tanh 2\theta_{k,z} = \frac{2f_z(k)}{d_z(k)}, \quad \tanh 2\theta_{k,\perp} = -\frac{2f_\perp(k)}{d_\perp(k)}, \tag{15}$$

where the longitudinal auxiliary functions f_z and d_z are defined by

$$f_z(k) = \frac{t\bar{s}^2}{4}\delta\gamma(k), \quad d_z(k) = \mu + \frac{2J_x - J_z}{4} + \frac{t\bar{s}^2}{2}\delta\gamma(k), \tag{16}$$

and for the in-plane case the auxiliary functions $f_\perp$ and $d_\perp$ are given by

$$f_\perp(k) = \frac{t\bar{s}^2}{4}\gamma(k), \quad d_{u,d}(k) = \mu + \frac{J_z}{4} + \frac{t\bar{s}^2}{2}\gamma(k) \pm \gamma_+,$$

$$d_\perp(k) = \frac{1}{2}(d_u + d_d) = \mu + \frac{J_z}{4} + \frac{t\bar{s}^2}{2}\gamma(k). \tag{17}$$

Here, $\gamma(k) = \Sigma_{i=1}^D \cos(k_i)$ with $\gamma(0) = \frac{z}{2}$ denotes the NN structure factor in dimension $D = \frac{z}{2}$ (z=coordination number of the simple cubic lattice). It should not be confused with the Zeeman energies $\gamma_\pm$ defined in Sec. III. The Bogoliubov transformations in Eqs. (13) and (14) yield the diagonalized bilinear Hamiltonian

$$\mathcal{H}_{mf} = E_0 + \sum_k [\Omega_A(k)A^\dagger(k)A(k) + \Omega_B(k)B^\dagger(k)B(k) + \Omega_z(k)a_k^\dagger a_k], \tag{18}$$

where the triplet-mode frequencies $\Omega_\alpha(k)$ ($\alpha = A,B,z$) in the mean-field Hamiltonian are given by

$$\Omega_A(k) = \omega_A(k) + \gamma_+,$$

$$\Omega_B(k) = \omega_B(k) - \gamma_+,$$

$$\Omega_z(k) = \omega_z(k),$$

$$\omega_A(k) = \omega_B(k) = [d_\perp(k)^2 - 4f_\perp(k)^2]^{1/2} \equiv \omega_\perp(k),$$

$$\omega_z(k) = [d_z(k)^2 - 4f_z(k)^2]^{1/2}. \tag{19}$$

The excitation energies $\Omega_\alpha(k)$ depend on the field, both explicitly through γ_+ (for $\alpha = A,B$) and implicitly via $\omega_\alpha(k)$ which is determined by the field-dependent singlet and triplet amplitudes. In the nonmagnetic phase ($\bar{u}, \bar{d}, \bar{t}_0 = 0$), the singlet-triplet excitation gap is given by the minimum excitation energy at the incipient ordering wave vector. For $D = 2$, this is at $Q = (\pi, \pi)$—explicitly, $E_g = \min\{\Omega_\alpha(Q), \alpha = A,B,z\}$. In the approach from the nonmagnetic side, the quantum critical line $t_c(h)$ is then defined by the vanishing of E_g.

The ground-state energy E_0 is a function of three control parameters $(t/J_x, \Delta, \delta)$, four singlet-triplet expectation values $(\bar{s}, \bar{t}_0, \bar{u}, \bar{d})$, and the chemical potential μ. Writing the transverse mean values explicitly in terms of amplitudes and phases according to

$$\bar{u} = u\exp(i\Phi_u), \quad \bar{d} = d\exp(i\Phi_d), \tag{20}$$

the ground-state energy can be written as

$$E_0\left(\frac{t}{J_x}, \Delta, \delta; \bar{s}, \bar{u}, \bar{d}, \bar{t}_0\right) = N\Bigg[-\frac{1}{4}(2J_x + J_z)\bar{s}^2 + \mu\bar{s}^2 - \mu + \left(\frac{J_z}{4} + \mu - \frac{1}{4}zt\bar{s}^2\right)(u^2 + d^2) + \gamma_+(u^2 - d^2) + \frac{z}{2}t\bar{s}^2 ud\cos(\Phi_u + \Phi_d) + \left(\frac{1}{4}(2J_x - J_z) + \mu + \frac{1}{2}z\delta t\bar{s}^2\right)\bar{t}_0^2 + 2\gamma_-\bar{s}\bar{t}_0\Bigg] + \frac{1}{2}\sum_{k\alpha}(\omega_k^\alpha - d_\alpha). \tag{21}$$

As a first step, we determine the triplet condensate phases (Φ_u, Φ_d) by minimization. Since only one term depends on the phases, we obtain the extremal condition $\sin(\Phi_u+\Phi_d)=0$. The minimum must also satisfy $\cos(\Phi_u+\Phi_d)<0$. This is achieved for $\Phi_u+\Phi_d=n\pi$ with n an odd integer; i.e., the sum is only determined modulo 2π. Since there is no condition for the difference of phases, one of them is arbitrary. We then choose $(\Phi_u, \Phi_d)=(0,\pi)$. The remaining continuous degeneracy with respect to the phase difference is a signature of the Goldstone mode which is present throughout the AF phase.

V. SELF-CONSISTENT EQUATIONS FOR SINGLET AND TRIPLET AMPLITUDES AND MAGNETIZATION

The minimization of the ground-state energy E_0 in Eq. (21) leads to self-consistent coupled equations for the condensate amplitudes $\bar{s}, \bar{u}, \bar{d}, \bar{t}_0$ and the chemical potential μ. Their structure is slightly different in the nonmagnetic ($\bar{t}=0$) and magnetic ($\bar{t}>0$) cases; therefore, we write them explicitly for both. For a convenient expression of the self-consistency equations, we define the quantity $\bar{\tau}_0$ by the relation $\bar{t}_0 \equiv \bar{\tau}_0 \bar{s}$. Furthermore, we introduce the Brillouin zone integrals F_α and G_α $(\alpha=A,B,z)$ given by

$$F_\alpha = \frac{1}{N}\sum_k \frac{d_\alpha(k)}{\omega_{k\alpha}},$$

$$G_\alpha = \frac{t}{N}\sum_k \frac{d_\alpha(k)-2f_\alpha(k)}{\omega_{k\alpha}}\gamma_k^\alpha, \tag{22}$$

which appear in the extremal conditions when differentiating the last term in E_0 with respect to μ or $\bar{s}$, respectively. Here, we have defined $\gamma_k^\perp \equiv \gamma_k^{A,B}=\gamma_k$ and $\gamma_k^z=\delta\gamma_k$. Note that even in the case of finite field $(\gamma_\pm \neq 0)$, it is the frequency $\omega_{k\alpha}$ and not the mode frequency $\Omega_{k\alpha}$ which appears in the expressions for F_α and G_α.

A. Nonmagnetic Kondo spin-singlet phase in an external field

In this case the transverse triplet amplitudes vanish—i.e., $u=d=0$—and the minimization of E_0 with respect to $(\bar{s}, \bar{t}_0 \equiv \bar{s}\bar{\tau}_0, \mu)$ leads to the self-consistent set of equations

$$\bar{s}^2 = \frac{\frac{1}{2}\left(5-\sum_\alpha F_\alpha\right)}{1+\bar{\tau}_0^2},$$

$$\bar{\tau}_0 = -\frac{2\gamma_-}{2\mu+\frac{1}{2}(2J_x-J_z)+z\delta t\bar{s}^2},$$

$$\mu = \frac{1}{2}\left[\left(J_x+\frac{1}{2}J_z\right)-\frac{1}{2}\sum_\alpha G_\alpha - 2\gamma_-\bar{\tau}_0 - z\delta t\bar{s}^2\bar{\tau}_0^2\right]. \tag{23}$$

Here, $\bar{s}$ and μ are found by iteration which determines $\bar{\tau}_0$ and hence $\bar{t}_0$ completely via the second equation above. For zero field—i.e., $\gamma_-=0$—the induced $\bar{\tau}_0$ vanishes and then Eq. (23) reduces to the paramagnetic case of Ref. 11.

B. Antiferromagnetic phase in an external field

The additional minimization with respect to u and d amplitudes leads to a direct relation for the chemical potential μ in terms of the singlet amplitude $\bar{s}$ which is a generalized version of the zero-field AF case:[11]

$$\mu(h) = \frac{1}{4}zt\bar{s}^2 - \frac{J_z}{4} + \left[\left(\frac{1}{4}zt\bar{s}^2\right)^2+\gamma_+^2\right]^{1/2}. \tag{24}$$

At this stage, it is convenient to introduce an auxiliary parameter κ which controls the effect of the external field on the boson amplitudes; it is defined by

$$\kappa(h) = \left[1+\left(\frac{\gamma_+}{\frac{z}{4}t\bar{s}^2}\right)^2\right]^{1/2}+\frac{\gamma_+}{\frac{z}{4}t\bar{s}^2}. \tag{25}$$

Obviously, $\kappa(0)=1$ and $\kappa(h)\leqslant 1$ since $\gamma_+<0$. Using the expression for the zero-field chemical potential $\mu_0=\mu(0)$, we may also write

$$\mu(h) = \mu_0 + \frac{z}{4}t\bar{s}^2\frac{(\kappa-1)^2}{2\kappa},$$

$$\mu_0 = \frac{z}{2}t\bar{s}^2 - \frac{1}{4}J_z. \tag{26}$$

We define a total transverse triplet amplitude $\bar{t}$ by $\bar{t}^2=\frac{1}{2}(u+d)^2$ which should not be confused with the hopping matrix element t of the Hamiltonian. The minimization with respect to u,d leads to a relation between the two amplitudes from which we obtain

$$u^2+d^2 = 2\bar{t}^2\frac{1+\kappa^2}{(1+\kappa)^2}, \quad u^2-d^2 = 2\bar{t}^2\left(\frac{1-\kappa}{1+\kappa}\right) \tag{27}$$

or, equivalently,

$$u^2 = \frac{2\bar{t}^2}{(1+\kappa)^2}, \quad d^2 = \frac{2\bar{t}^2\kappa^2}{(1+\kappa)^2} = \kappa^2u^2. \tag{28}$$

The remaining set of singlet and triplet amplitudes $(\bar{s}, \bar{t}, \bar{t}_0 = \bar{s}\bar{\tau}_0)$ is again determined by the solution of three coupled equations

$$\bar{s}^2 = \frac{\frac{1}{2}\left(5-\sum_\alpha F_\alpha\right)-(u^2+d^2)}{1+\bar{\tau}_0^2},$$

$$\bar{\tau}_0 = -\frac{2\gamma_-}{2\mu+\frac{1}{2}(2J_x-J_z)+z\delta t\bar{s}^2} \equiv -2\gamma_-\hat{\tau}_0,$$

$$\bar{t}^2 = \frac{1}{zt}\left[2\mu - \frac{1}{2}(2J_x + J_z) + 2\gamma_- \bar{\tau}_0 + \frac{1}{2}\sum_\alpha G_\alpha\right] + \delta\bar{s}^2\bar{\tau}_0^2. \tag{29}$$

These amplitudes are related to the spin expectation values by

$$\langle S_z\rangle = \bar{s}\bar{t}_0 + \frac{1}{2}(u^2 - d^2),$$

$$\langle \tau_z\rangle = -\bar{s}\bar{t}_0 + \frac{1}{2}(u^2 - d^2). \tag{30}$$

For zero field ($\bar{\tau}_0 = 0$), the system of equations (29) may be shown to reduce to the one already discussed in Ref. 11. In this case, $\kappa = 1$ and $u = d$—i.e., circularly polarized triplet modes with equal amplitudes.

Finally, we discuss the uniform magnetization M_0 and the staggered magnetization $M_s = M_B = -M_A$ associated with AF order. By definition

$$M_0 = g_s\langle S_z\rangle + g_\tau\langle \tau_z\rangle,$$

$$M_s = g_s\langle S_x^B\rangle + g_\tau\langle \tau_x^B\rangle. \tag{31}$$

Here, the staggered moment is assumed to be polarized along x. Using the expressions in Eq. (30) for $\langle S_z\rangle$, $\langle \tau_z\rangle$, and similar ones for $\langle S_x\rangle$ and $\langle \tau_x\rangle$, we obtain with the help of Eqs. (25) and (27)

$$M_0 = \bar{s}\bar{t}_0\left[2g_- + 2g_+\lambda\left(\frac{\bar{t}^2}{\bar{s}\bar{t}_0}\right)\right] \simeq 2g_-\bar{s}\bar{t}_0 \equiv 2g_- m_0,$$

$$M_s = \bar{s}\bar{t}\left[2g_- - 2g_+\lambda\left(\frac{\bar{t}_0}{\bar{s}}\right)\right] \simeq 2g_-\bar{s}\bar{t} \equiv 2g_- m_s. \tag{32}$$

Here, we used $g_\pm = \frac{1}{2}(g_s \pm g_\tau)$ and defined

$$\lambda = \frac{1-\kappa}{1+\kappa}. \tag{33}$$

When both staggered and uniform component are nonzero, the total magnetic moment is canted. The canting angle α, counted from the xy plane is then given by

$$\tan\alpha = \left(\frac{\bar{t}_0}{\bar{t}}\right)\frac{g_- + g_+\lambda\left(\frac{\bar{t}^2}{\bar{t}_0\bar{s}}\right)}{g_- - g_+\lambda\left(\frac{\bar{t}_0}{\bar{s}}\right)}. \tag{34}$$

The terms $\sim\lambda$ are higher-order corrections—e.g., $\sim(h/J_x)^2$ for M_s. For moderate fields, they may be neglected. In Sec. VII (Fig. 4), we only show the main contribution $m_s \equiv \bar{s}\bar{t}$ in accordance with Ref. 11. In Eq. (34) a similar small field approximation may be employed for the canting angle leading to $\alpha \simeq \tan^{-1}(\bar{t}_0/\bar{t})$. For equal g factors $g_s = g_\tau$ ($g_- = 0$ and $\bar{t}_0 = 0$), one has a special case $M_s = 0$ due to moment compensation of local and itinerant spins, although this is still a phase with an AF order parameter $m_s = \bar{s}\bar{t}$. The uniform moment M_0 is now given by $M_0 = 2g_+\lambda\bar{t}^2$, oriented parallel to the external field ($\alpha = \pi/2$).

C. Ground-state energy: Condensation versus fluctuation

It is instructive to rewrite the ground-state energy in a different way which renders a clearer interpretation of its individual contributions. The total mean-field Hamiltonian in Eq. (18) may be rewritten as

$$\mathcal{H}_{mf} = \tilde{E}_0 + \sum_{\alpha=z,A,B}\sum_k \Omega_\alpha(k)\left(n_\alpha + \frac{1}{2}\right), \tag{35}$$

where n_α is the occupation number of bosons for each mode. The total ground-state energy is then given by

$$E_0 = \tilde{E}_0 + \frac{1}{2}\sum_{k\alpha}\Omega_\alpha(k), \tag{36}$$

where $\tilde{E}_0(h)$ consists of three parts according to

$$\tilde{E}_0/N = -\left[\frac{1}{4}(2J_x + J_z)\left(\bar{s}^2 + \frac{1}{2}\right) + \mu\left(\frac{5}{2} - \bar{s}^2\right)\right] + \frac{z}{2}t(\kappa-1)^2\bar{s}^2\bar{t}^2 + \left(\frac{1}{4}(2J_x - J_z) + \mu + \frac{z}{2}\delta t\bar{s}^2\right)\bar{t}_0^2 + 2\gamma_-\bar{s}\bar{t}_0. \tag{37}$$

Here, the first part ($\tilde{E}_0$) in Eq. (36) is the condensate contribution. The second always positive term is due to triplet quantum fluctuations. According to Eq. (37), $\tilde{E}_0$ is composed of three parts: The first (negative) contribution is due to the singlet formation. The second (positive) part is due to the field-induced triplet polarisation. The last term is the Zeeman energy contribution. For zero field only, the first term in Eq. (37) is present.[11] The ground state with $E_0 < 0$ will be determined by the competition of these terms. For example, when $h = 0$ the quantum critical point where AF order appears will be determined by the balance of two terms: The negative singlet formation energy and the positive energy of triplet quantum fluctuations.

VI. INFLUENCE OF HIGHER-ORDER TERMS

The transformation of the Hamiltonian in Eq. (1) to bond operator variables also creates third- and fourth-order terms in the triplet operators. They have been neglected in the previous analysis based on Eqs. (6) and (7). In fact, it was argued in Ref. 11 that third-order terms do not contribute to the ground-state energy and fourth-order terms are quantitatively negligible. The latter was also found for the related bilayer Heisenberg model.[22] Hence, higher-order terms have no influence on the zero-field quantum critical properties. In this section, we investigate to what extent this is still justified in the presence of an external field. Indeed, in the mean-field approximation used here, the higher-order terms lead to field-induced effective bilinear triplet terms which have to be added to the genuine bilinear term in Eq. (11) which is present already at zero field. The quantitative influence of

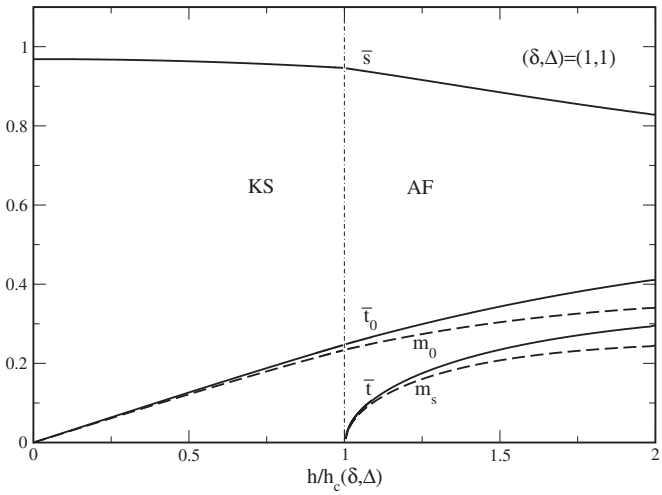

FIG. 2. Singlet ($\bar{s}$) and triplet ($\bar{t}_0, \bar{t}$) amplitudes and their associated uniform ($m_0=\bar{s}\bar{t}_0$) and staggered ($m_s=\bar{s}\bar{t}$) moments as a function of field strength normalized to the critical field in the KS and AF regions. Here, $h_c(\delta,\Delta)/J_x=0.55$. At the critical field $(\bar{t}_0/\bar{s})=0.25$. This case with $t/t_c(\delta,\Delta)=0.6$ $(t/J_x=0.517)$ corresponds to the upper curve of Fig. 4 (top). Here $(g_s,g_\tau)=(2.0)$.

higher-order terms on $t_c(h)$ or $h_c(t)$ is controlled by the ratio $(\bar{t}_0/\bar{s})$ at the critical field h_c where $\bar{t}_0(h_c)$ is the field-induced triplet amplitude. If it is still moderate compared to the singlet amplitude $\bar{s}(h_c)$, then higher-order terms have negligible influence. The field dependence of these amplitudes as obtained from Eqs. (23) and (29) is shown in Fig. 2 for a typical case.

The contribution of third order in $t_{n\alpha}$ (n=site, $\alpha=x,y,z$) to the interaction term is given by[11]

$$\mathcal{H}_1^{(3)} = \frac{it}{4}\sum_{\langle n,m\rangle}[(s_n^\dagger t_{nx} + t_{nx}^\dagger s_n)(t_{my}^\dagger t_{mz} - t_{mz}^\dagger t_{my}) + (s_n^\dagger t_{ny} + t_{ny}^\dagger s_n) \times (t_{mz}^\dagger t_{mx} - t_{mx}^\dagger t_{mz}) + \delta(s_n^\dagger t_{n,z} + t_{n,z}^\dagger s_n)(t_{m,x}^\dagger t_{m,y} - t_{m,y}^\dagger t_{m,x})], \tag{38}$$

which has to be added to Eq. (8). We are only interested in the influence of this term on the quantum critical lines $h_c(t)$ or $t_c(h)$ to be discussed in Sec. VII. As explained there, this may be achieved both from the paramagnetic (KS) and AF side of the critical line. Here, we consider only the former for reasons explained at the end of the section. In this case the circular triplet amplitudes $\bar{u}=\bar{d}\equiv 0$. The mean-field approximation to $H_1^{(3)}$ then contains only terms proportional to $\bar{t}_0$, and no constant contribution to E_0 appears. Transforming these terms into circular triplet coordinates, one finally obtains another bilinear contribution with

$$\mathcal{H}_{1mf}^{(3)} = -\frac{t}{4}z\delta\bar{s}\bar{t}_0\sum_n (u_n^\dagger u_n - d_n^\dagger d_n) + \frac{t}{2}\bar{s}\bar{t}_0\sum_{\langle nm\rangle}(u_n^\dagger u_m - d_n^\dagger d_m). \tag{39}$$

This contribution is field induced since for small fields $\bar{t}_0(h)\sim h$. The first single site term in Eq. (39) has the same structure as the γ_+ part of the Zeeman term and may be accommodated by a simple (nonlinear) rescaling of the applied field such that γ_+ is replaced by $\tilde{\gamma}_+$ according to

$$\tilde{\gamma}_+(h) = -g_+ h f_s(h), \quad f_s(h) = 1 + \frac{z}{4}\delta t\frac{\bar{s}(h)\bar{t}_0(h)}{h}. \tag{40}$$

Here, $f_s(h)$ is the rescaling function for the applied field. Note that for $\delta=0$ one has $f_s(h)\equiv 1$; i.e., no rescaling will occur in this case. The second contribution in Eq. (39) is an interaction to which the same (transverse) Bogoliubov transformation as before may be applied. These terms then have a simple effect: In Eq. (17) one has to replace $d_{u,d}(k) \to d_{u,d}(k) \pm (t/2)\bar{s}\bar{t}_0\gamma(k)$. However, only the average $d_\perp(k) = [d_u(k)+d_d(k)]/2$ of the auxiliary functions, which is unchanged, enters the expression for $\omega_{A,B}(k)$ in Eq. (19). Therefore $\omega_{A,B}(k)$ is also unchanged by the third-order contribution. As a result the total energy E_0 in Eq. (21) will be exactly the same as before. Also the self-consistent equations (23) will be unchanged. Note that in these equations γ_- is not rescaled. The only effect of the third-order terms is therefore the above rescaling of the external field in the γ_+ Zeeman term leading to the modified transverse-mode frequencies

$$\tilde{\Omega}_{A,B}(k) = \omega_{A,B}(k) \pm \tilde{\gamma}_+. \tag{41}$$

Therefore the critical field h_c of the quantum phase transition which is defined as the field where one of the above modes $[\tilde{\Omega}_+(k)$ for $h>0]$ vanishes at the AF wave vector $\mathbf{Q}=(\pi,\pi)$ will be changed by the scaling factor $f_s(h_c)$. If h_c^0 is the critical field without third-order terms, then approximately $h_c=h_c^0/f_s(h_c^0)$ is the critical field with the effect of third-order terms included. This is only a quantitative modification which we will discuss in Sec. VII in connection with Fig. 5. The qualitative topology of the phase diagram will not be changed by the third-order term. We note again that in the special case $(\Delta,\delta)=(\Delta,0)$, the third-order term does not have any effect at all because $f_s\equiv 1$. Furthermore, for all cases $g_s=g_\tau$, there is no field-induced triplet amplitude—i.e., $\bar{t}_0\equiv 0$ according to Eq. (23), leading again to $f_s\equiv 1$. We conclude that the influence of third-order terms is not important for the field-induced quantum critical behavior.

Now, we discuss the effect of terms which are of fourth order in the triplet operators. They are given by[11]

$$\mathcal{H}_1^{(4)} = \frac{-t}{4}\sum_{\langle n,m\rangle}[(t_{ny}^\dagger t_{nz} - t_{nz}^\dagger t_{ny})(t_{my}^\dagger t_{mz} - t_{mz}^\dagger t_{my}) + (t_{nx}^\dagger t_{nz} - t_{nz}^\dagger t_{nx}) \times (t_{mx}^\dagger t_{mz} - t_{mz}^\dagger t_{mx}) + \delta(t_{nx}^\dagger t_{ny} - t_{ny}^\dagger t_{nx})(t_{mx}^\dagger t_{my} - t_{my}^\dagger t_{mx})]. \tag{42}$$

The mean-field approximation to $H^{(4)}$ for the nonmagnetic case $(\bar{u}=\bar{d}=0)$ does not produce a constant term but leads to an effective bilinear contribution in circular triplet coordinates:

$$\mathcal{H}_{1mf}^{(4)} = \frac{t}{2}\bar{t}_0^2 \sum_{\langle nm \rangle} \left(u_n^\dagger u_m + d_n^\dagger d_m + \frac{1}{2}(u_n d_n + d_n u_m + u_n^\dagger d_m^\dagger + d_n^\dagger u_m^\dagger) \right). \quad (43)$$

Again, this is a field-induced bilinear contribution with $\bar{t}_0(h) \sim h^2$ for small fields. Due to $\bar{u}, \bar{d}=0$, it has no longitudinal part. It may be diagonalized by the same transverse Bogoliubov transformation in Eq. (14) as before. The new mode frequencies including fourth-order contributions are simply obtained by the replacement $\tilde{d}_\perp = d_\perp + (t/2)\bar{t}_0^2\gamma(k)$ and $\tilde{f}_\perp = f_\perp - (t/4)\bar{t}_0^2\gamma(k)$ in Eq. (17). This will lead to the modified transverse frequency

$$\tilde{\omega}_{A,B}(k)^2 = \omega_{A,B}(k)^2 \left(1 + \bar{t}_0^2 \frac{t\gamma(k)}{d_\perp - 2f_\perp} \right) \quad (44)$$

and new mode frequencies $\tilde{\Omega}_{A,B}(k) = \tilde{\omega}_{A,B}(k) \pm \gamma_+$ At the quantum critical point where $\tilde{\Omega}_A(Q)=0$, this may be approximately written as

$$\tilde{\omega}_{A,B}(k) \simeq \omega_{A,B}(k) \left[1 + \frac{1}{z} \left(\frac{\bar{t}_0}{\bar{s}} \right)_c^2 \gamma(k) \right], \quad (45)$$

where the index c denotes the values of singlet and triplet amplitudes at the QCP. From Fig. 2, we can estimate that the prefactor in Eq. (45) is of the order $\frac{1}{z}\left(\frac{\bar{t}_0}{\bar{s}}\right)^2 \simeq 10^{-2}$ since at the QCP the triplet amplitude is still quite small and the singlet amplitude basically unchanged from the zero-field value. Therefore, the fourth-order terms lead to corrections of the order 1% in the frequencies $\omega_{A,B}(k)$ which determine the last term in the ground-state energy of Eq. (21). Indeed, the correction to E_0 is even smaller since the momentum summation over $\omega_{A,B}(k)$ in the last term of Eq. (21) leads to a large amount of cancellation because $\gamma(k)$ is positive in one-half of the Brillouin zone and negative in the other half. Therefore, the self-consistent equations for $\bar{s}$ and $\bar{t}_0$ are nearly unchanged and we can conclude that the field-induced quantum critical behavior is not influenced by the inclusion of fourth-order terms. Our analysis shows that the quantum critical lines $h_c(t)$ are only marginally influenced by the presence of higher-order terms in one example and have no effect in other cases. However, for fields with $h \gg h_c$ one would expect that the higher-order terms should lead to non-negligible corrections, at least in the case of third-order contributions. From Fig. 2, one can see that for $h/h_c > 2$, the ratio $(\bar{t}_0/\bar{s})$ approaches 0.5 and the bilinear approximation might become inadequate. In fact, by its very construction the bond-operator method is a strong coupling theory which assumes the dominance of the singlet state. It cannot be expected to be quantitatively correct for high fields when saturation of moments is approached—i.e., when singlet and triplet amplitudes become equal. In this limit, it is more appropriate to start from the polarized canted state and perform a conventional spin-wave expansion for the two types of spins.

As a consequence of the above analysis, we will only consider the genuine bilinear Hamiltonian, Eq. (11), as used in the previous sections for the following numerical calculations. This restriction has an additional reason: Although the critical $h_c(t)$ or $t_c(h)$ may be calculated by searching for the vanishing of the excitation gap E_g from the nonmagnetic singlet side, it is more satisfactory to search also from the AF magnetic side for the vanishing of the staggered magnetization m_s and confirm the agreement. This cannot be done easily when third- and fourth-order terms are included. On the AF side, the latter lead, to a mixing of the longitudinal and transverse modes and a closed analytic form of the Bogoliubov transformation cannot be found. Therefore, it is better to include only the bilinear terms and be aware of the trivial effect of field rescaling by the third-order terms and the tiny effect of fourth-order terms. This standpoint will be adopted for the following numerical analysis.

VII. NUMERICAL SOLUTION FOR EXCITATION GAP AND AF ORDER PARAMETER, CRITICAL FIELD CURVES, AND THE *H-T* PHASE DIAGRAM

We shall now discuss the numerical solutions of the self-consistent equations (23) and (29) which describe the AF-KS quantum phase transitions—i.e., the field dependence of the Kondo singlet gap E_g and the field dependence of the staggered magnetization m_s. The former was defined below Eq. (19) and the latter in Eq. (32). We shall only discuss the results for $D=2$ and $\delta \leqslant 1$—i.e., the easy xy-plane situation with $\mathbf{m}_s \perp c$. In this case, $\Omega_{A,B}(k) \leqslant \Omega_z(k)$. As shown before, the qualitative behavior of $D=3$ is similar to $D=2$ (Ref. 11). The main purpose is to study the dependence of the quantum critical point (QCP) $t_c(h)$ on the external field or, equivalently, the dependence of the quantum critical field $h_c(t)$ on the hopping strength t. To check consistency, the QCP has been obtained both by variation of t and of h and both from the paramagnetic ($E_g=0$) as well as the antiferromagnetic ($m_s=0$) side of the QCP. As mentioned in the previous section, this requires restriction to the genuine bilinear Hamiltonian terms.

Before discussing the field dependent results, we show the behavior of the quantum critical $t_c(\Delta, \delta)$ as function of the anisotropies in the zero-field case as a starting point of our analysis. The calculation of $t_c(\Delta, \delta)$ has been described in Ref. 11. Here, we present the results for the full range of anisotropies (Fig. 3) from the U(1)-xy case via Heisenberg-SU(2) to Ising-Z_2 symmetry. Note the two different scales on the left (J_x) and right (J_z) half of each part of Fig. 3. The quantum critical t_c for the KS-AF transition reaches a singular maximum for the Heisenberg case and generally vanishes for the Ising case, except for $\delta=0$. This may be understood by comparing with Fig. 1. For $\Delta \to \infty$ (i.e., $\Delta' \to 1$), the two singlets with $S_z^t=0$ become degenerate and an arbitrary small interaction t leads to the AF state. However, for $\delta=0$ the $S_z^t=0$ states are not connected by a matrix element of $\mathcal{H}_1^{(2)}$ and, hence, AF can occur only via matrix elements between the singlet ground state and the excited doublet which requires a finite $t_c/J_x=0.35$ for AF order to occur.

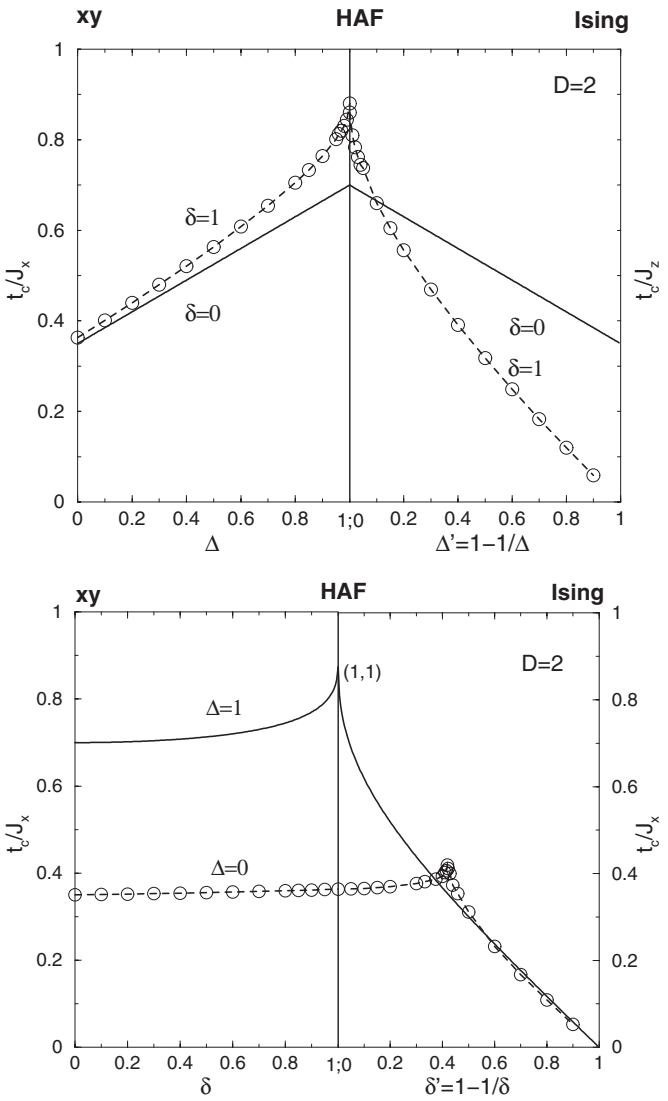

FIG. 3. Critical hopping strength $t_c(\delta,\Delta)$ for quantum phase transition between Kondo singlet ($t<t_c$) and antiferromagnetic ($t>t_c$) phases at zero field. For $(\delta,\Delta)=(0,\Delta)$ or $(\delta,1)$, t_c is obtained from a closed analytical expression [Eq. (25) in Ref. 11] (solid lines); for the other cases, it is calculated from the zero-field version of Eq. (23) (dashed lines). Top: t_c dependence on anisotropy Δ of local spins. In the Ising case ($\Delta'\to 1$), t_c for $\delta=0$ does not vanish because the AF order is due to the mixing with the doublet separated by a finite excitation gap. Bottom: t_c dependence on anisotropy δ of interacting spins. The value $t_c(0,1)/J_x=0.7$ agrees with results from Monte Carlo simulatons for the genuine Kondo lattice model in two dimensions (Refs. 20 and 21).

The effect of the external field for $(g_s,g_\tau)=(2,0)$ is shown in Fig. 4 (top), for the two cases $(\Delta,\delta)=(0,0)$ (○) and (1,1) (◇). Their corresponding t_c values may be taken from Fig. 3. In Fig. 4 (top) we choose a subcritical value $t/t_c(\Delta,\delta)=0.6$, meaning a nonmagnetic singlet phase with finite E_g exists for zero field. When the field is increased, the gap is gradually reduced until it is closed at $t_c(h_c)$. For the (normalized) t value of 0.6, obviously, the difference in critical fields h_c is not significant. However, the qualitative behavior of the spin gap E_g in the two cases for $h<h_c$ is different with a much smaller slope of E_g in the xy case as compared to the Heisenberg case. In both cases for $h>h_c$ a field-induced easy-plane AF order parameter appears—i.e., a phase sequence KS-AF for increasing field. The opposite behavior is observed in the genuine KN case $(\Delta,\delta)=(1,0)$ with $(g_s,g_\tau)=(2,0)$ in Fig. 4 (bottom). For an above-critical value $t/t_c(0,1)=1.1(t/J_x=0.77)$ the AF order parameter is gradually suppressed until it vanishes at $h_c/J_x=1.23$ and the Kondo singlet phase appears; i.e., the opposite phase sequence AF-KS is realized. Finally, for slightly subcritical $t/t_c(0,1)=0.94$ $(t/J_x=0.658)$ an interesting reentrance sequence KS-AF-KS of phases as function of field is observed. It exists only in a narrow range of subcritical values $0.91<t/t_c<1.0$. As discussed in Sec. VI, this behavior is robust because third-order triplet contributions are exactly zero for $\delta=0$.

We may collect the data of quantum critical fields h_c from numerous calculations such as presented in Fig. 4 and similar ones for quantum critical t_c at fixed h in an h-t phase diagram. It is shown in the form of $t_c(h)$ curves in Fig. 5 for two choices of the g factors. For $(g_s,g_\tau)=(2,0)$ and the cases $(\Delta,\delta)=(0,0),(1,1)$, the scaled $t_c(h)$ is identical close to the zero-field QCP; i.e., the slope does not depend on the anisotropy (Δ,δ). For larger fields, one observes the plateau formation in the case $(\Delta,\delta)=(1,1)$ and the further monotonic decrease for $(\Delta,\delta)=(0,0)$. This behavior may qualitatively be understood from the field dependence of the local energy levels of $\mathcal{H}_J$ shown in Fig. 1. For increasing h, the gap between the ground state and first excited state decreases and hence a smaller t_c is necessary to achieve the softening of the triplet excitation at Q. For $\Delta=1$, this effect eventually levels off because the splitting of the two lowest local levels becomes constant at large field and approaches $2\Delta J_x$ so that $t_c(h)$ reaches a plateau at large fields for nonzero Δ. On the other hand, for $\Delta=0$ the two lowest levels become asymptotically degenerate and hence $t_c(h)$ should approach zero for large fields. As already noted in the discussion of Fig. 4, the intermediate case $(\Delta,\delta)=(1,0)$ and $(g_s,g_\tau)=(2,0)$ behaves quite differently. After an initial but much weaker decrease of $t_c(h)$, it reaches a minimum at $(h/J_x,t/J_x)=(0.275,0.638)$ and then starts to increase again. The region of the nonmonotonic behavior with slightly subcritical $t/t_c(0,1)$ corresponds to the region where reentrance behavior KS-AF-KS is observed in Fig. 4. For above-critical $t/t_c(0,1)$, once $t_c(h)>t$ the initial AF phase is suppressed and we obtain the sequence AF-KS—i.e., a field-induced KS phase corresponding to Fig. 4 (bottom). In all three cases with $(g_s,g_\tau)=(2,0)$ one has a finite $t_c(h)$ for finite fields.

This is different if we chose equal g factors $(g_s,g_\tau)=(2,2)$. For this choice the lowest two local levels cross at $h=0.25$ $(\Delta=0)$ and at $h=0.5$ $(\Delta=1)$ (not shown in Fig. 1). This is due to the fact that S^t_z commutes with the Hamiltonian and hence there is no level repulsion of the two $S^t_z=0$ states. Consequently, at this point, the quantum critical $t_c(h)$ vanishes in all three cases of (Δ,δ). It decreases essentially linearly from its maximum value at $h=0$. The phase diagram in Fig. 5 shows a collection of the critical $t_c(h)$ curves for the six cases considered. The corresponding gapped KS- and AF-ordered phases are below and above each curve, respec-

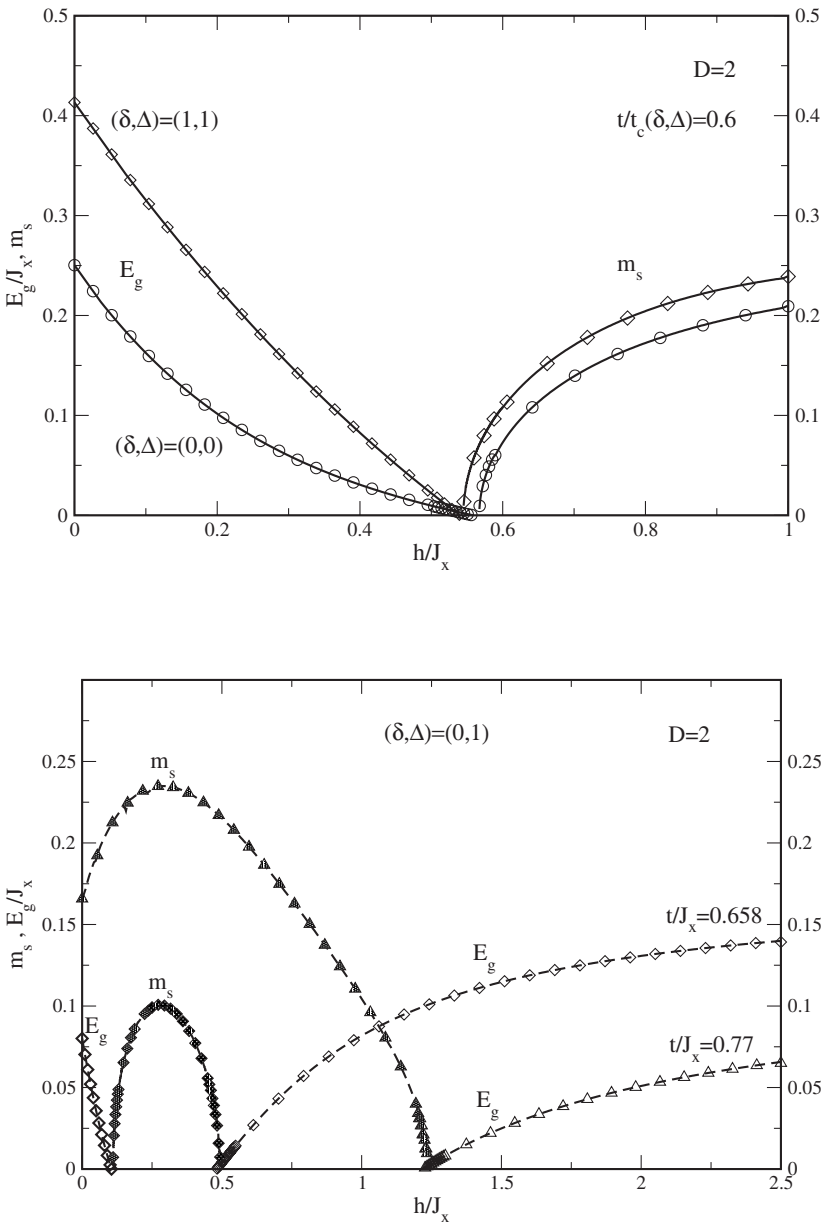

FIG. 4. In these figures three possible cases for quantum phase transitons between Kondo singlet KS (E_g=singlet gap) and antiferromagnetic AF (m_s=staggered moment) phases as a function of increasing field strength h are shown: (i) Field-induced AF with sequence KS-AF. (ii) Destruction of AF and field-induced gap opening corresponding to the sequence KS-AF. (iii) Reentrant behavior corresponding to KS-AF-KS. Top: singlet-triplet excitation gap E_g and AF order parameter m_s as a function of external field for the two cases $(\delta,\Delta)=(0,0)$ (circles) and $(\delta,\Delta)=(1,1)$ (diamonds) as a function of the external field. A subcritical scaled value $t/t_c(\delta,\Delta)=0.6$ is used in both cases $[t_c(0,0)/J_x=0.350,\ t_c(1,1)/J_x=0.862]$. Here, $(g_s,g_\tau)=(2,0)$ is used. This plot corresponds to the field-induced AF case (i). Bottom: similar plot for $(\delta,\Delta)=(0,1)$ and an above critical $t/t_c(\delta,\Delta)=1.1$ $(t/J_x=0.77)$ and subcritical $t/t_c(\delta,\Delta)=0.94$ $(t/J_x=0.658)$. In the former case (ii), one has the sequence AF-KS of phases ($\triangle$) and in the latter (iii) a reentrant situation with KS-AF-KS sequence is observed ($\diamond$).

tively. We comment again on the influence of third-order terms discussed in Sec. VI on the phase diagram of Fig. 5. Remembering that all cases with $\delta=0$ or $g_s=g_\tau$ are unaffected by the third-order contributions, only one of the critical field curves in Fig. 5 [$\star$ $(g_s,g_\tau)=(2,0)$] may be influenced. In this case, third-order terms lead to an almost field-independent and moderate rescaling of h_c by a factor ~ 1.2 according to Eq. (40) and Fig. 2.

Finally, in Fig. 6 we show the dependence of the tilting angle of the total moment out of the xy plane for two possible cases with AF order. It is calculated from Eq. (34) (solid line) and a simplified (low-field) expression given in the caption. Close to the quantum critical field the staggered moment vanishes and the total moment is then aligned with the external field ($\|z$), meaning $\alpha=\pi/2$.

VIII. DISCUSSION

As we have mentioned in the Introduction, the interest in the Kondo necklace model stems from two facts: (i) it is thought to be a simplified version of the original Kondo lattice model with itinerant electrons and (ii) it is expected to describe some basic features of the observed quantum phase transitions in real Kondo materials. Although there is no mapping or exact equivalence of the two models, the agreement of their qualitative features by simply identifying the intersite interaction (KN) and hopping (KL) energies (both given by t) is generally quite good. As discussed in Refs. 11 and 17, the 1D Kondo necklace model does not exhibit quantum critical behavior; this agrees with earlier numerical work on the KL model[23] where the disordered spin-gapped state always prevails.[7]

We discussed the more interesting 2D case where quantum phase transitions in the KN model are possible.[11,17] One can compare the values of the quantum critical t_c/J (we set $J=J_x$ in this section to comply with literature conventions) obtained for the KN model from Fig. 3 with those for the KL model obtained in Monte Carlo (MC) simulations obtained previously.[20,21,24] In the spirit of Doniach's replacement in

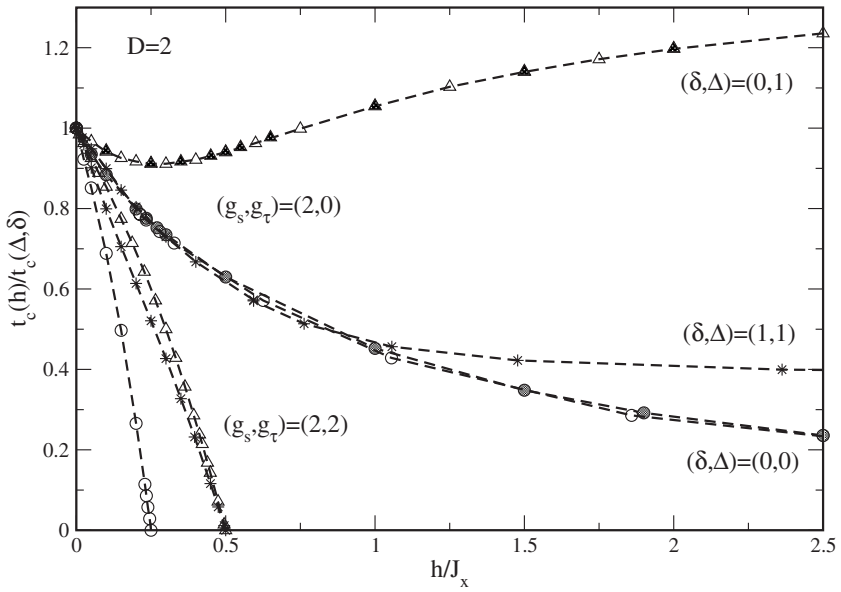

FIG. 5. *t-h* phase diagram [critical $t_c(h)$ curves] for various cases of anisotropies (δ,Δ) and *g* factors (g_s,g_τ). Here, circles (○) correspond to $(\delta,\Delta)=(0,0)$, stars (⋆) to $(\delta,\Delta)=(1,1)$, and triangles (Δ) to $(\delta,\Delta)=(0,1)$. Solid symbols are obtained by $m_s=0$ from the AF side, open symbols by $E_g=0$ from the Kondo singlet side. For unequal *g* factors, the Heisenberg case shows saturation at $t_c/J_x\simeq 0.4$ at larger fields; in the Ising case, t_c continues decreasing. For the mixed case, $(\delta,\Delta)=(0,1)$ (the genuine KN model in 2D) and unequal *g* factors the $t_c(h)$ is nonmonotonic. In each case, the KS phase is below and the AF phase above the corresponding $t_c(h)$ curve. A decreasing $t_c(h)$ leads to the phase sequence KS-AF (field-induced AF) whereas an increasing $t_c(h)$ entails the opposite sequence AF-KS. In the nonmonotonic region, the reentrance behavior KS-AF-KS is observed. For comparison see Fig. 4. For equal *g* factors in all cases, t_c decreases monotonically and vanishes at rather small fields.

1D we should compare with the KN model for *xy*-type interactions—i.e., with the $(\delta,\Delta)=(0,1)$ case in Fig. 3 which has a $t_c/J=0.7$. The MC simulations for the 2D SU(2) fermionic KL model lead to quantum critical parameters (average values) $t_c/J=0.71$,[20] 0.69,[21,24] and 0.68,[16] very close to the appropriate value in Fig. 3 (upper panel, center of solid line; lower panel, left corner of solid line). Note that the critical t_c's corresponding to solid lines in Fig. 3 are obtained from a simple analytical formula within the bond-operator mean-field approach.[11] Further support for this scenario comes from exact-diagonalization (ED) results for the KL model on small clusters[25] using open boundary conditions. The total average local moment $\langle\mu_{loc}^2\rangle=\langle(\boldsymbol{\tau}_i+\mathbf{S}_i)^2\rangle$ calculated as function of J/t shows a reduction to half of the free moment size due to Kondo singlet formation in the lattice for the value $t_c/J=0.67$. If it is interpreted as the critical value in the thermodynamic limit, this is again close to the above results. This near equality of analytical KN and numerical KL results seems to suggest that even in 2D the SU(2) KL model is better described by the U(1) *xy*-type KN model with $(\delta,\Delta)=(0,1)$ since the SU(2) KN model with $(\delta,\Delta)=(1,1)$ has a considerably larger critical value $t_c/J=0.862$.

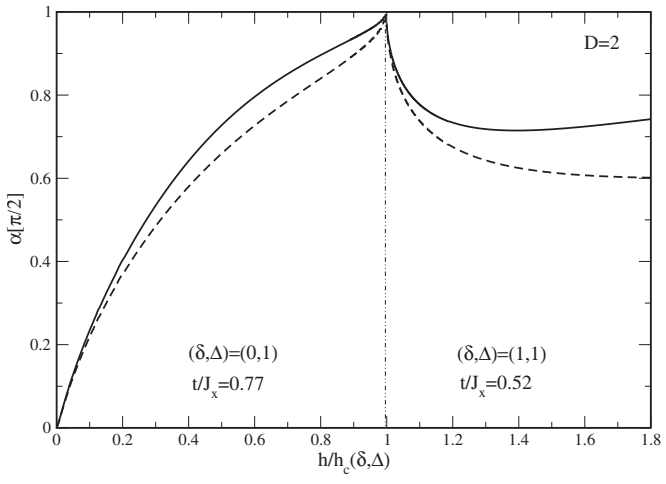

FIG. 6. Canting angle α of total moment moment (counted from the *xy* plane) in the AF phase of two different cases (cf. Fig. 4) with $(g_s,g_\tau)=(2,0)$. Solid curve is obtained from the exact expression, Eq. (34), and dashed curve from the approximate expression $\alpha\simeq\tan^{-1}(\bar{t}_0/\bar{t})$. At the quantum critical field h_c, the staggered moment vanishes and the total moment is aligned with the external field $(\alpha=\pi/2)$. Here, $h_c(0,1)/J_x=1.23$ and $h_c(1,1)/J_x=0.55$.

The fermionic KL model is obtained from the periodic Anderson model (PAM) by a Schrieffer-Wolff transformation which eliminates charge fluctuations of *f* electrons. The resulting Kondo coupling *J* is then given in terms of the Anderson model parameters by $J=-UV/\epsilon_f(\epsilon_f+U)$ where $\epsilon_f<0$ is the *f*-level position with respect to the Fermi level at zero energy, *U* is the on-site *f*-electron repulsion, and *V* is their hybridization strength with conduction electrons. The periodic Anderson model may be studied with the dynamical mean-field theory (DMFT).[26] This method has been used more recently to investigate its quantum critical properties[27] which should be related to those of the Kondo lattice and hence also KN models. The method is formally a $D=\infty$ approximation but has nevertheless been used for studying electron correlations in finite-dimensional lattices such as the

3D PAM in Ref. 27. Using the value of J from the Schrieffer-Wolff transformation the extrapolated $T=0$ phase diagram suggests that the critical hopping strength at the QCP is given by $t_c/J \simeq 0.43$. This is again in reasonable agreement with the mean-field bond-operator result for the 3D KN model which predicts $t_c/J=0.38$.[11]

While the quantum critical behavior as function of control parameter t/J is well presented, there are few microscopic investigations concerning the field-induced quantum critical behavior of KL- and KN-type models such as provided here. The fermionic 2D KL model in an external field with equal g factors corresponding to $(g_s,g_\tau)=(2,2)$ was studied in Ref. 16 by using variational and MC methods. The numerical results for $J/t=3$ suggest that the transition between Kondo- and AF-ordered regime takes place in a field region ($B \equiv 2h$ in notation of Ref. 16) between $B_c^-/t=1.0$ and $B_c^+/t=2.25$. In this regime, both Kondo-like features and transverse magnetic order coexist. From the present calculations of the 2D KN model again with $(\delta,\Delta)=(0,1)$, g factors as above and using the data shown in Figs. 3 and 5 one obtains $B_c/t=1.86$ ($B_c/J=0.62$) which is close to the average 1.63 of the above $B_c^{\pm}/t$ values. This value for the critical field was also confirmed by ED results for the KL model on small clusters[25] where the breaking up of on-site singlet formation was observed above the value $B_c/J \simeq 0.5$. We conclude that KL and KN models also seem to exhibit similar field-induced quantum critical behavior. Another matter is the scaling behavior of singlet gap and staggered magnetization around the critical field. The present mean-field-type theory does not give sufficient insight into that issue. It has so far been treated within continuum field theories involving order parameter fluctuations around the critical field.[28]

The present bond-operator mean-field results for the KN model are apparently consistent with known numerical results for the fermionic Kondo lattice models. It is less clear whether they are useful for the interpretation of experimental results, especially for the field-induced quantum phase transitions. Since charge degrees of freedoms are eliminated in the KN model, it is, strictly speaking, more appropriate for the Kondo-insulator compounds which have a hybridization gap due to half-filled conduction bands. However, we ignore this subtlety in the following and also apply it to the magnetism of metallic Kondo compounds. The zero-field quantum critical behavior as a function of the control parameter t/J can experimentally be mimicked by applying hydrostatic or chemical pressure (by substitution of elements). This changes mostly the hybridization and hence the Kondo coupling J. In the accessible pressure regime, one may assume that t/J varies linearly with pressure. In this manner, it is feasible to drive AF-ordered heavy fermion systems to the quantum critical point where they become nonmagnetic heavy Fermi liquids. Since hydrostatic (positive) pressure generally increases J, it tends to suppress the AF phase while with suitable substitution of elements (negative) chemical pressure may decrease J which favors AF order. Thus the AF QCP may be approached from both sides. There are many examples to be found especially among Ce compounds; for a review, see Ref. 29. In most cases of Ce compounds, however, the AF QCP may not be reached directly because it is enveloped by a "dome" of the superconducting phase and the critical pressure has to be obtained from extrapolation to $T=0$. While the KL- and KN-type models discussed above naturally suggest the AF QCP, there is no direct way of experimental determination of the critical $(t/J)_c$ since its relation to the experimentally accessible critical pressure p_c (or critical concentration of substituent) is unknown. In fact, most of the interest on pressure-induced QCPs focuses more on the scaling exponents of various quantities with respect to the distance $(p-p_c)$ to the QCP. This is extensively discussed in the reviews cited in the Introduction.

For the field-induced quantum phase transition, much less experimental results are available. A review of materials investigated is given in Ref. 30. A recent example of a field-induced destruction of AF order is the tetragonal $YbRh_2Si_2$ compound.[31] At ambient pressure and zero field, it has an AF order which is indeed of the easy-plane (xy)-interaction type ($\delta=0$). The AF order is destroyed at 0.66 T for field along the hard c axis and a nonmagnetic Fermi liquid state appears above the critical field. If one assumes that the local Kondo interaction which results from the Schrieffer-Wolff mechanism is more of the isotropic nature ($\Delta=1$), it qualitatively corresponds to the AF-KS scenario shown in the lower panel of Fig. 4. As mentioned before the reentrant scenario shown also in this figure exists only in a narrow parameter range and it is perhaps understandable that no such example is known. What is really surprising is the following observation: Most of the parameter cases in Fig. 5 would predict the KS-AF sequence—i.e., the field-induced AF order out of the Kondo phase. This is a natural consequence that in most cases a field reduces the singlet-triplet gap and supports the onset of magnetic order as shown in the upper panel of Fig. 4. We would like to stress that this is also the only phase sequence found in the fermionic KL model.[16] However, field-induced AF magnetic order is not easily found in heavy fermion compounds. For example, $CeNi_2Ge_2$ at ambient pressure and zero field is in the Kondo singlet phase and rather close to the AF quantum phase transition which may be achieved by appropriate substitution of Ni. Thus, it is a complementary case to $YbRh_2Si_2$. However, in an external field, there is no field-induced transition to transverse AF order as one might naively expect from the model discussion; rather, it is driven further away from the AF QCP as specific heat and resistivity measurements suggest.[31] There is, however, one known example of a heavy fermion system which exhibits field-induced AF order, though complicated by the appearance of superconductivity. The compound $CeRhIn_5$ is already an AF at ambient pressure.[32] Application of hydrostatic pressure moves it to the nonmagnetic (KS) side where it also becomes superconducting. Additional application of a magnetic field destroys the superconductivity and leads to the reestablishment of a field-induced AF order in a wide range of pressure from 1.4 to 2.4 GPa.[32] This is indeed the KS-AF sequence of phases corresponding to Fig. 4 (top) which appears in the majority of cases studied here. Experimentally, however, it seems to be the one most rarely encountered.

These examples suggest that while the Kondo-lattice- or necklace-type models have some qualitative and instructive properties which are relevant for magnetic quantum phase

transitions, they may not be able to explain some experimental observations in heavy fermion compounds. It is well possible that the complete elimination of charge degrees of freedom is too radical by suppressing hybridization effects of moments with conduction electrons and thus favoring the magnetic phases. Therefore, the more fundamental PAM model, including appropriate local and conduction electron Zeeman terms, may be a more promising starting point for future investigations of field-induced quantum phase transitions in heavy fermion compounds.

IX. CONCLUSION AND OUTLOOK

In this work, we have investigated the general anisotropic Kondo necklace model and its quantum phase transition from paramagnetic singlet phase to AF phase and vice versa in an external field. We have derived a bosonic Hamiltonian using the bond-operator representation of local and interacting spins and diagonalized the bilinear part by a generalized Bogoliubov transformation to circular polarized modes to include the effect of the external field. Higher-order parts of the Hamiltonian were found to be insignificant for the quantum critical behavior. In the mean-field approximation, one obtains a total ground-state energy that depends on the singlet amplitude $\bar{s}$, staggered and uniform triplet amplitudes $\bar{t},\bar{t}_0$, and the chemical potential. Minimization leads to two sets of self-consistent equations for Kondo singlet and AF phases, respectively.

From their numerical solution, we find that in most investigated cases the t_c value of the quantum critical point decreases monotonously with field strength leading to the KN-AF phase sequence for increasing field. In the case of unequal g factors and $(\Delta,\delta)=(1,1)$, it levels off at a plateau value $t_c(h)/t_c(\Delta,\delta)\simeq 0.4$ while for $(\Delta,\delta)=(0,0)$, it continues to decrease at larger field. However, for the genuine KN case with $(\Delta,\delta)=(1,0)$ the $t_c(h)$ curve is nonmonotonic with a minimum at $h/J_x\simeq 0.275$ at small fields and continues to increase for larger fields. Depending on the size of t, this implies two possibilities: For above critical t a suppression of AF and the opening of a spin excitation gap for $h>h_c$ (AF-KN sequence) or the reentrance behavior (KN-AF-KN sequence) of the gapped singlet phase for slightly subcritical t [as compared to $t_c(0)$]. For equal g factors, a crossing of local levels occurs due to a conserved S_z^t and the critical t_c reaches zero already at relatively small fields for all investigated cases of (δ,Δ). Since our treatment is of mean-field type, we will get mean-field exponents for the spin gap E_g and magnetization m_s at the field-induced QCP. This is apparent from Fig. 4 and has not been discussed further. Improvement for the critical exponents will require a self-consistent renormalization theory for the triplet excitations close to the quantum critical point.

ACKNOWLEDGMENTS

The authors would like to thank V. Yushankhai for helpful suggestions. A.L. would like to acknowledge the support of Sharif University of Technology. A.L. also would like to acknowledge the Max Planck Institute for the Physics of Complex Systems, Dresden, where the initial part of this work was started during his visit.

[1] M. A. Continentino, Braz. J. Phys. **35**, 197 (2005).
[2] M. Continentino, *Quantum Scaling in Many-body Systems* (World Scientific, Singapore, 2001).
[3] S. Sachdev, *Quantum Phase Transitions* (Cambridge University Press, Cambridge, England, 1999).
[4] M. Vojta, Rep. Prog. Phys. **66**, 2069 (2003).
[5] P. Fulde, P. Thalmeier, and G. Zwicknagl, in *Solid State Physics*, edited by H. Ehrenreich and F. Spaepen (Academic Press, Amsterdam, 2006), Vol. 60.
[6] S. Doniach, Physica B **91**, 231 (1977).
[7] H. Tsunetsugu, M. Sigrist, and K. Ueda, Rev. Mod. Phys. **69**, 809 (1997).
[8] I. Zerec, B. Schmidt, and P. Thalmeier, Physica B **378–380**, 702 (2006).
[9] I. Zerec, B. Schmidt, and P. Thalmeier, Phys. Rev. B **73**, 245108 (2006).
[10] T. Yamamoto, K. Ide, and C. Ishii, Phys. Rev. B **66**, 104408 (2002).
[11] A. Langari and P. Thalmeier, Phys. Rev. B **74**, 024431 (2006).
[12] V. N. Kotov, O. Sushkov, Zheng Weihong, and J. Oitmaa, Phys. Rev. Lett. **80**, 5790 (1998).
[13] Ch. Brünger and F. F. Assaad, arXiv:cond-mat/0605396 (unpublished).
[14] T. Schork, S. Blawid, and J.-I. Igarashi, Phys. Rev. B **59**, 9888 (1999).
[15] P. Gegenwart, J. Custers, C. Geibel, K. Neumaier, T. Tayama, K. Tenya, O. Trovarelli, and F. Steglich, Phys. Rev. Lett. **89**, 056402 (2002).
[16] K. S. D. Beach, P. A. Lee, and P. Monthoux, Phys. Rev. Lett. **92**, 026401 (2004).
[17] G.-M. Zhang, Q. Gu, and L. Yu, Phys. Rev. B **62**, 69 (2000).
[18] S. Sachdev and R. N. Bhatt, Phys. Rev. B **41**, 9323 (1990).
[19] T. Yamamoto, R. Manago, Y. Mori, and C. Ishii, J. Phys. Soc. Jpn. **72**, 3204 (2003).
[20] Z. Wang, X.-P. Li, and D.-H. Lee, Physica B **199–200**, 463 (1994).
[21] F. F. Assaad, Phys. Rev. Lett. **83**, 796 (1999).
[22] Y. Matsushita, M. P. Gelfand, and C. Ishii, J. Phys. Soc. Jpn. **68**, 247 (1999).
[23] R. T. Scalettar, D. J. Scalapino, and R. L. Sugar, Phys. Rev. B **31**, 7316 (1985).
[24] S. Capponi and F. F. Assaad, Phys. Rev. B **63**, 155114 (2001).
[25] I. Zerec, B. Schmidt, and P. Thalmeier, J. Magn. Magn. Mater. **310**, e48 (2007).
[26] M. Jarrell, H. Akhlaghpour, and Th. Pruschke, Phys. Rev. Lett. **70**, 1670 (1993).
[27] P. Sun and G. Kotliar, Phys. Rev. Lett. **95**, 016402 (2005).
[28] I. Fischer and A. Rosch, Phys. Rev. B **71**, 184429 (2005).

[29] P. Thalmeier, G. Zwicknagl, O. Stockert, G. Sparn, and F. Steglich, in *Frontiers in Superconducting Materials*, edited by A. V. Narlikar (Springer, Berlin, 2005).
[30] G. R. Stewart, Rev. Mod. Phys. **73**, 797 (2001).
[31] P. Gegenwart, J. Custers, T. Tayama, K. Tenya, C. Geibel, G. Sparn, N. Harrison, P. Kerschl, D. Eckert, K.-H. Müller, and F. Steglich, J. Low Temp. Phys. **133**, 3 (2003).
[32] T. Park, F. Ronning, H. Q. Yuan, M. B. Salamon, R. Movshovich, J. L. Sarrao, and J. D. Thompson, Nature (London) **440**, 65 (2006).